



EXPLICIT EQUIVALENT FORCE CONTROL FOR REAL-TIME SUBSTRUCTURE TESTING

H. Zhou¹, B. Wu², T. Wang³, D. Wagg⁴, M. Li⁵, J. Dai⁶

1 Postdoctoral Fellow, Institute of Engineering Mechanics, China Earthquake Administration, PR China.

E-mail: zhouhuimeng@iem.ac.cn

2 Professor, Dept. of Civil Engineering, Harbin Institute of Technology, PR China

3 Professor, Institute of Engineering Mechanics, China Earthquake Administration, PR China.

4 Professor, Dept. of Mechanical Engineering, University of Sheffield, United Kingdom.

5 Research Assistant, Institute of Engineering Mechanics, China Earthquake Administration, PR China.

6 Professor, Institute of Engineering Mechanics, China Earthquake Administration, PR China.

ABSTRACT

This paper employs the equivalent force control (EFC) method to solve the velocity difference equation in a real-time substructure test, which uses feedback control loops to replace the mathematical iteration to solve the nonlinear dynamic equation. The spectral radius analysis of amplification matrix shows that the EFC combined with explicit Newmark- β method has good numerical characteristics. Its stability limit of $\Omega=2$ remains unchanged regardless of the system damping, because the velocity is perfectly achieved during simulation. Compared with the proposed method, the stability limits of the central difference method using direct velocity prediction and the EFC-average acceleration method with linear interpolation decrease with the increase of system damping. The unconditionally stable EFC-average acceleration method even becomes to be conditionally stable. If an over-damped system with a damping ratio of 1.05 is considered, the stability limit is $\Omega=1.45$. Finally, an experiment of single degree of freedom structure installed with magneto-rheological (MR) damper was carried out demonstrating that the proposed method is able to track both displacement and velocity commands accurately, thus performing good applicability and accuracy for velocity-sensitive structures.

KEYWORDS: *Real-time substructure test; EFC; Velocity control; Explicit Newmark- β method; Stability*

1. GENERAL INSTRUCTIONS

In real-time substructural tests, hydraulic servo loading systems are usually displacement-controlled. As the displacement of the specimen reaches the command displacement, the velocity usually doesn't reach the target velocity and the acceleration control has worse performance. When the experimental substructure is a velocity dependent component, the measured reaction force is inaccurate, so the precision of the test is affected. In real-time substructural tests, explicit integration methods [1-5] are widely used because of the simple calculation. However, the traditional explicit integration methods [1] are implicit to velocity while they are explicit to displacement. Wu *et al.* [6] improved the traditional central difference method using the forward difference to obtain the explicit equation of the velocity. Although this method has a decrease in the stability limit compared to the traditional central difference method, the accuracy of the velocity is increased, and open-loop control of velocity can be achieved. Darby *et al.* proposed a method using input signal integral to smooth the displacement command, so that better speed response can be achieved. This method can merely make the response smoother but it can not assure perfect tracking of velocity. In order to perform real-time substructural tests of damper specimens, Wu *et al.* [8] used the linear interpolation of equivalent force command and achieved a better accuracy of the velocity control. In order to improve the velocity control accuracy for real-time substructural testing, EFC using explicit Newmark- β algorithm is proposed in this paper. Different from the interpolation and smoothing methods that have been referred to, velocity tracking control in an integration time interval is ensured by using close-loop control method, so that the accuracy of the velocity response is guaranteed.

2. EXPLICIT EQUIVALENT FORCE CONTROL METHOD

Consider a structure like Fig. 2.1, in a real-time substructural test there are a numerical substructure and an experimental substructure. The mass, damping and the stiffness matrices of the numerical substructure are

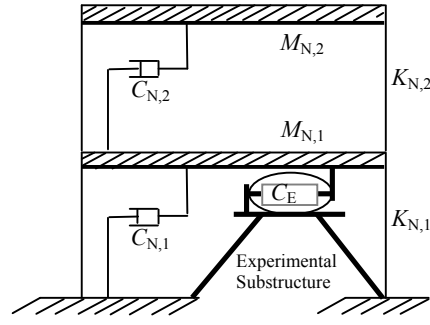


Figure 2.1 Block diagram of the RST with damper specimen

by M_N , C_N and K_N . Subscript N indicates that the vector is relative to the numerical substructure. Subscript E indicates that the vector is relative to the experimental substructure. The corresponding inertial force, damping force and restoring force have been obtained in simulation. The experimental substructure is a velocity dependent opponent, the restoring force of which is represented by f_s and is the function of displacement and velocity. Thus the equation of motion for an real-time hybrid test can be expressed in a more general and precise form as

$$M_N \mathbf{a} + \mathbf{R}_N(\mathbf{v}) + K_N \mathbf{d} + \mathbf{f}_s(\mathbf{v}, \mathbf{d}) = \mathbf{p} \quad (1)$$

where \mathbf{d} , \mathbf{v} , \mathbf{a} are respectively the vector of displacement, velocity, acceleration, \mathbf{p} is the external load vector, and \mathbf{R} is the damping force.

The dynamic Eq. (1) is discretized in time domain and the explicit Newmark- β method is used to solve the equation, as shown in Eq. (2) - (4):

$$M_N \mathbf{a}_{k+1} + K_N \mathbf{d}_{k+1} + \mathbf{R}_N(\mathbf{v}_{k+1}) + \mathbf{f}_s(\mathbf{v}_{k+1}, \mathbf{d}_{k+1}) = \mathbf{p}_{k+1} \quad (2)$$

$$\mathbf{v}_{k+1} = \mathbf{v}_k + \frac{\Delta t}{2} (\mathbf{a}_k + \mathbf{a}_{k+1}) \quad (3)$$

$$\mathbf{d}_{k+1} = \mathbf{d}_k + (\Delta t) \mathbf{v}_k + \frac{1}{2} (\Delta t)^2 \mathbf{a}_k \quad (4)$$

where Δt is the integration time interval. Eq. (3) can be written as

$$\mathbf{a}_{k+1} = \frac{(2\mathbf{v}_{k+1} - 2\mathbf{v}_k - \Delta t \mathbf{a}_k)}{\Delta t} \quad (5)$$

Substituting Eq. (4) and Eq. (5) into Eq. (2), the following Equation is obtained.

$$C_{PD} \mathbf{v}_{k+1} + \mathbf{R}_N(\mathbf{v}_{k+1}) + \mathbf{f}_s(\mathbf{v}_{k+1}, \mathbf{d}_{k+1}) = \mathbf{F}_{EQ,k+1} \quad (6)$$

in which

$$C_{PD} = \frac{2M_N}{\Delta t} \quad (7)$$

$$\mathbf{F}_{EQ,k+1} = \mathbf{p}_{k+1} - K_N \mathbf{d}_k + \frac{2M_N - K_N \Delta t^2}{\Delta t} \mathbf{v}_k + (M_N - \frac{1}{2} K_N \Delta t^2) \mathbf{a}_k \quad (8)$$

Eq. (6) can be viewed as a hybrid dynamic equilibrium condition. $\mathbf{R}_N(\mathbf{v}_{k+1})$ on the left side of the equation is the damping force of the numerical substructure. $C_{PD} \mathbf{v}_{k+1}$ can be loosely interpreted as the pseudodamping force for the entire system, and the third term is the total (i.e. dynamic plus static) the resistance developed by the experimental substructure. The term $\mathbf{F}_{EQ,k+1}$ on the right side of the Eq. (6) can be considered as an equivalent external force exerted to the hybrid system, which can be determined by the step $k+1$ excitation force exerted to the hybrid system and the structural state \mathbf{a}_k ,

v_k , d_k . The solution of Eq. (6) is the response of the hybrid system to the equivalent external force. The basic framework of this method is the same with implicit equivalent force control method [8], while the difference is that the solution of Eq. (6) is the velocity v_{k+1} , and the solution of the equation in the implicit equivalent force control method is displacement d_{k+1} .

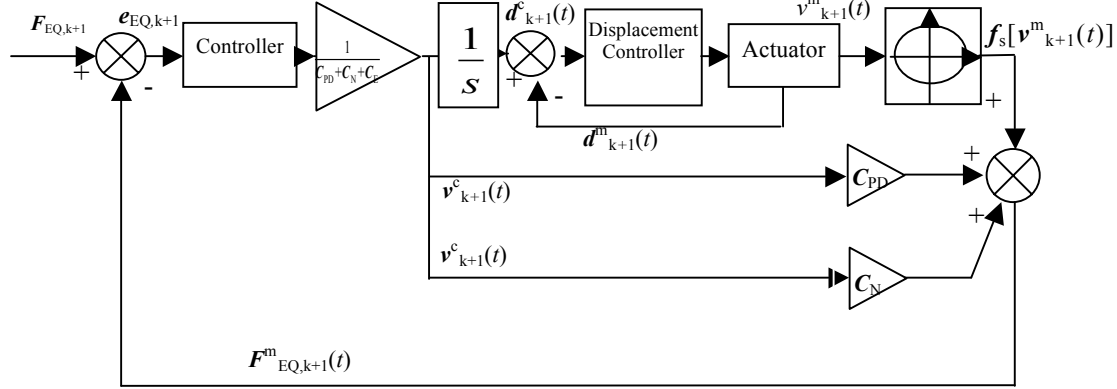


Figure 2.2 Block diagram of the explicit EFC method

Based on the analysis above, the principle of explicit equivalent force control method is shown as Fig. 2.2. During each integration time interval Δt , the equivalent force command $F_{EQ,k+1}(t)$ is a function of the time, the equivalent force error $e_{EQ,k+1}$ pass through the equivalent force controller, and by multiplying its output with $(C_{PD} + C_N + C'_E)^{-1}$ the velocity command $v^c_{k+1}(t)$ is obtained. The displacement command $d^c_{k+1}(t)$ is obtained through the integrating unit s^{-1} from the velocity command, so that the loading system works in the traditional displacement-controlled mode during a real-time substructure test. $(C_{PD} + C_N + C'_E)^{-1} s^{-1}$ is defined as conversion matrix C_F , where C'_E is the initial damping coefficient. Constants can be employed in the conversion matrix C_F , which can be obtained from the initial structural state by calculating the derivative of Eq. (6) with respect to d_{k+1} . For nonlinear experimental structures, the test results will be affected if C_F is constant. By properly designing the equivalent force controller, e.g. designing the controller using sliding mode control method [9], the affection of the values of C_F can be weakened. $f_s[v^m_{k+1}(t)]$ and $v^m_{k+1}(t)$ are respectively the reaction force response and velocity response of the experimental substructure under the displacement command $d^c_{k+1}(t)$. $F^m_{EQ,k+1}(t)$ is the feedback of the equivalent force. It is to be noticed that $f_s[v^m_{k+1}(t)]$ is relative to $v^m_{k+1}(t)$. If the equivalent force response can accurately track the equivalent force command, the velocity $v^c_{k+1}(t)$ will be very close to the target velocity v_{k+1} when the integration time interval Δt ends.

Of course it is to be noted that the velocity v_{k+1} at the end of every integration time interval is difficult to measure from the experimental substructure and needs to be calculated from Eq. (6) with the measured reaction force $R_N[v^c_{k+1}]$ of the numerical substructure and $f_s[v^m_{k+1}(t)]$ of the experimental substructure in the explicit equivalent force control method. Because the control error is unavoidable in feedback control, it causes actuator displacement error in the meantime. And the composite filters^[10] are applied to obtain velocity response from displacement response and acceleration response in this paper, velocity response error is also inevitable.

3. NUMERICAL STABILITY OF EXPLICIT EQUIVALENT FORCE CONTROL METHOD

The numerical stability of explicit equivalent force control method is analyzed using a single degree of freedom of structure as an example. Partial damping of the single degree of freedom structure is used as the experimental substructure, and the damping force is assumed to be linear. Eq. (6) can be rewritten as

$$C_{PD}v_{k+1} + C_N v_{k+1} + C_E v_{k+1} = F_{EQ,k+1} \quad (9)$$

where C_{PD} and C_N respectively represent the pseudodamping coefficient and the damping coefficient of the numerical substructure, C_E is the damping coefficient of the experimental substructure. At the end of the integration time interval, assuming that the velocity of the experimental substructure reaches steady state and satisfies Eq. (9), the steady velocity v_{k+1} can be obtained as Eq. (10). Substituting Eq. (10) into Eq. (5), assuming the structure is in free vibration, Eq. (11) is obtained. Define X_{k+1} and Eq. (13) is obtained. By Eq. (12), Eq. (4),

Eq. (3), and the numerical substructure damping C_N is $\mathbf{0}$, the amplification matrix \mathbf{A} can be obtained as Eq. (14).

$$v_{k+1} = \frac{F_{EQ}}{C_{PD} + C_E + C_N} \quad (10)$$

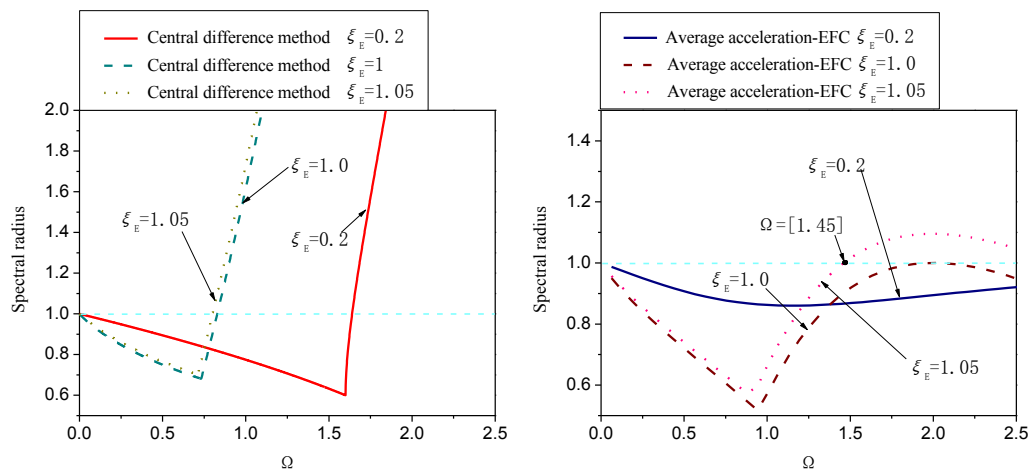
$$a_{k+1} = \frac{-K_N d_k - (C_N + C_E + K_N \Delta t) v_k - 0.5 \Delta t a_k (C_N + C_E + K_N \Delta t)}{M_N + 0.5 \Delta t (C_N + C_E)} \quad (11)$$

$$\mathbf{X}_{k+1} = [d_{k+1}, \Delta t v_{k+1}, \Delta t^2 a_{k+1}] \quad (12)$$

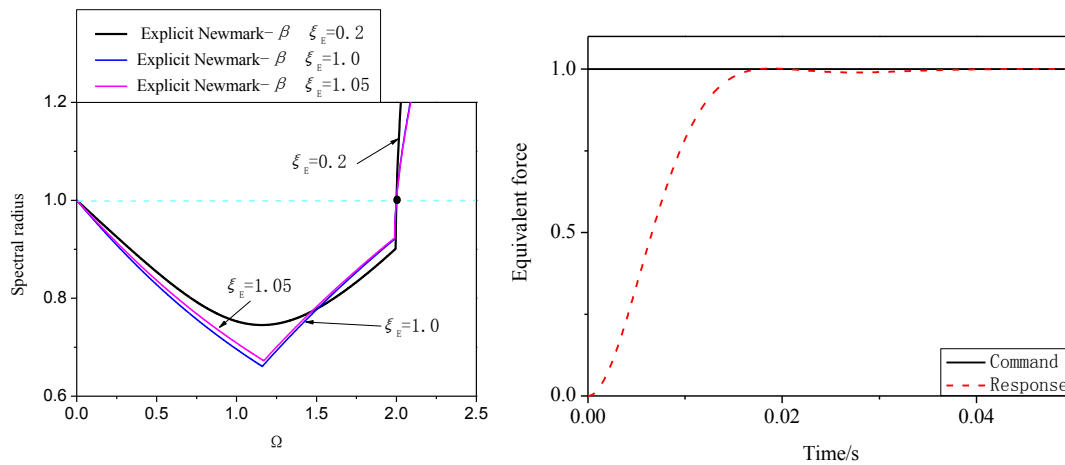
$$\mathbf{X}_{k+1} = \mathbf{A} \mathbf{X}_k \quad (13)$$

$$\mathbf{A} = \begin{bmatrix} 1 & 1 & \frac{1}{2} \\ \frac{-\frac{1}{2} \Omega^2}{1 + \xi_E \Omega} & \frac{1 - \frac{1}{2} \Omega^2}{1 + \xi_E \Omega} & \frac{\frac{1}{2} - \frac{1}{4} \Omega^2}{1 + \xi_E \Omega} \\ \frac{-\Omega^2}{1 + \xi_E \Omega} & \frac{-2 \xi_E \Omega - \Omega^2}{1 + \xi_E \Omega} & \frac{-\xi_E \Omega - \frac{1}{2} \Omega^2}{1 + \xi_E \Omega} \end{bmatrix} \quad (14)$$

where $\Omega = \omega \Delta t$, ω is the circular frequency of the structure, and ξ_E is the damping ratio of the experimental substructure. When the stability condition of numerical integration is satisfied: spectral radius $\rho(\mathbf{A}) \leq 1$; the stability range of explicit EFC in this paper is $\Omega \leq 2$. The comparison with the central difference method and average acceleration equivalent force control method with linear interpolation is shown below in Fig. 3.1.



a) Central difference method with direct velocity prediction b) EFC-average acceleration method



c) Explicit EFC

Figure 3.1 Spectral radius analyzing

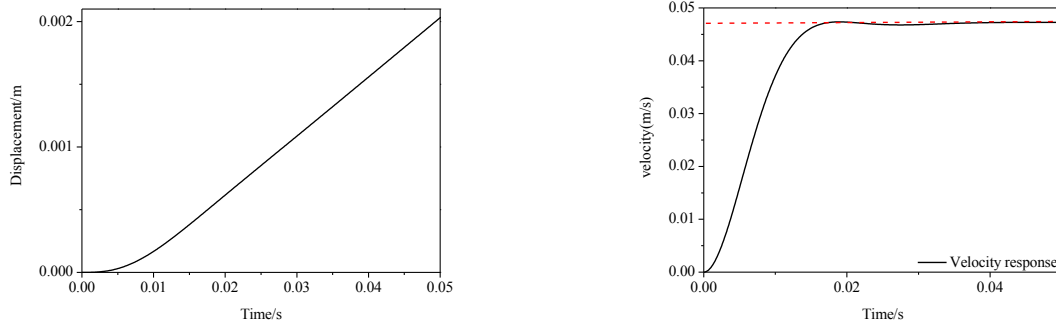
Figure4.1 Equivalent force response with step input

It can be seen from Fig. 3.1 a) that the stability limit of the real-time substructure central difference method decreases comparing to the traditional central difference method due to the velocity assumption. As the explicit EFC method directly uses control method to obtain the speed, thus the numerical stability of the integration algorithm is maintained, and the stability limit is $\Omega=2$ regardless of the damping ratio, so it has good numerical characteristics. The unconditional stability of the average acceleration equivalent force control method [8] is lost after the equivalent force command linear interpolation is delivered. As is shown in Fig. 3.1 b), when the damping ratio of the experimental substructure is very large, e.g. when $\zeta_E=1.05$, its stability limit changes to $\Omega=1.45$. The stability of the explicit equivalent force control method excels that of the interpolation force control method based on average acceleration method at this point. It is worthy to be noted that the accuracy of the velocity measurement in the explicit EFC influences the precision of the equivalent control, thus when error exists in the velocity measurement it is likely to lead to error in displacement. So this method is suitable for testing dampers with damping force as a major component and with smaller stiffness.

5. NUMERICAL SIMULATION ANALYSIS

Numerical simulation is carried out for the single degree of freedom structure. The parameters of the structure are: $M_N=720\text{kg}$, $K_N=74404\text{N/m}$, $K_E=0\text{N/m}$, $\zeta_N=0.05$, $M_E=0$, $\zeta_E=0.05$. The natural frequency of the structure is 1.6179Hz . The transfer function model of the actuator-specimen system is $T_A(s) = \omega_A^2 (s^2 + 2\zeta_A \omega_A s + \omega_A^2)^{-1}$, where the parameters $\zeta_A=0.8$, $\omega_A=316.14\text{rad/s}$. The parameters of the outer controller of the equivalent force controller are $k_p=0.41$, $k_i=140$.

The equivalent force response and displacement response of unit step input are shown in Fig. 4.1 and Fig. 4.2. The unit step response of the equivalent force and the velocity track the command satisfactorily, and the displacement response is ramp response, which is also consistent with the theoretical results.



a) Displacement response

b) Velocity response

Figure 4.2 Step response of displacement and velocity

The structural parameters and the actuator model are the same parameters as Fig. 4.2. The parameters of the PI controller are: $k_p=1$, $k_i=60$. Polynomial prediction compensation algorithm^[11] is applied, which uses polynomial interpolation to obtain the new equivalent force command

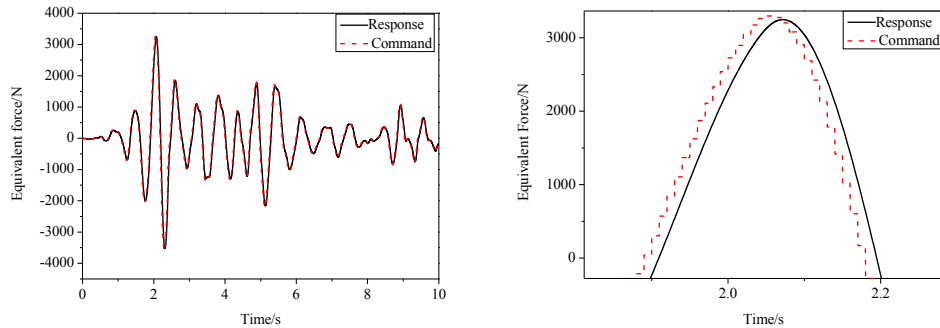
$$F'_{EQ,P+1} = \begin{bmatrix} 1 & P\Delta t & L & (P\Delta t)^N \end{bmatrix} \mathbf{a} = F_{EQ,k+P+1} \quad (15)$$

where P is the forward prediction step, \mathbf{a} is the coefficient matrix obtained by least square fitting from the equivalent force command of former n steps.

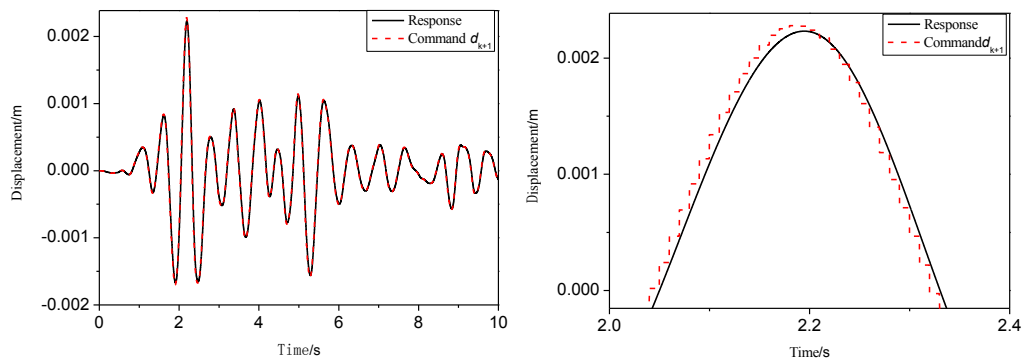
$$\mathbf{a} = \begin{bmatrix} a_0 \\ a_1 \\ M \\ a_N \end{bmatrix} = \mathbf{X}^{-1} \mathbf{F}_{EQ} = \begin{bmatrix} 1 & 0 & L & 0 \\ 1 & -\Delta t & L & (-\Delta t)^N \\ M & M & M & M \\ 1 & -(n-1)\Delta t & L & (-(n-1)\Delta t)^N \end{bmatrix}^{-1} \begin{bmatrix} F_{EQ,k+1} \\ F_{EQ,k} \\ M \\ F_{EQ,k-n+2} \end{bmatrix} \quad (16)$$

The parameters in Eq. (15) and Eq. (16) were chosen as: $N=4$, $n=5$, $P=1.2$, $\Delta t = 0.01$. El-Centro earthquake acceleration was input. The peak value of the acceleration was 12.5gal . The equivalent force, displacement and velocity responses are shown in Fig. 4.3, Fig. 4.4 and Fig. 4.5. It can be seen from Fig. 4.3 that the equivalent

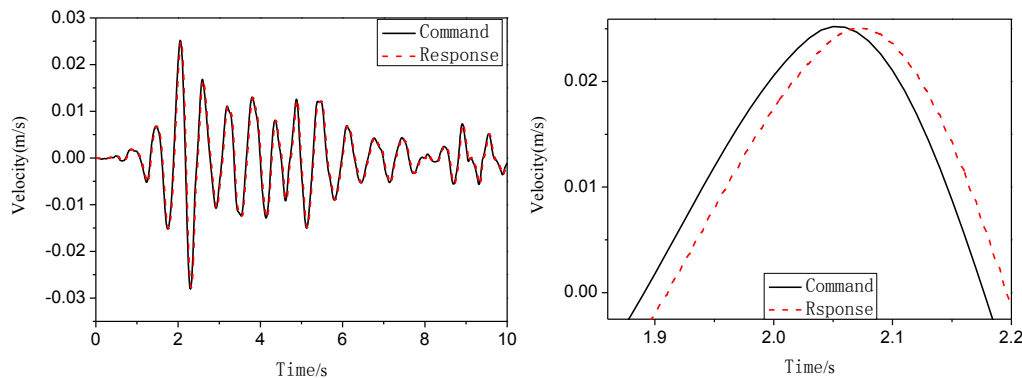
force response tracks the equivalent force command accurately. It is proved that the equivalent force controller has good performance. It can also be seen from Fig. 4.4 and Fig. 4.5 that the displacement response and the velocity response of the damper specimen agree respectively with the displacement command d_{k+1} and the velocity command v_{k+1} . It is demonstrated that this method can guarantee the implementation of the displacement commands and speed commands from the numerical simulation.



a) Equivalent force response b) Enlarged view of Equivalent force response
 Figure 5.3 Equivalent force response with damper specimen



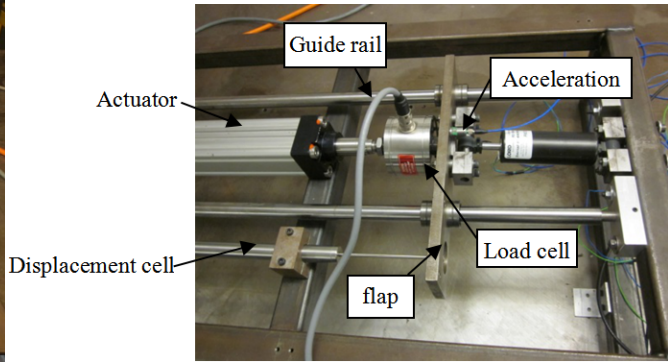
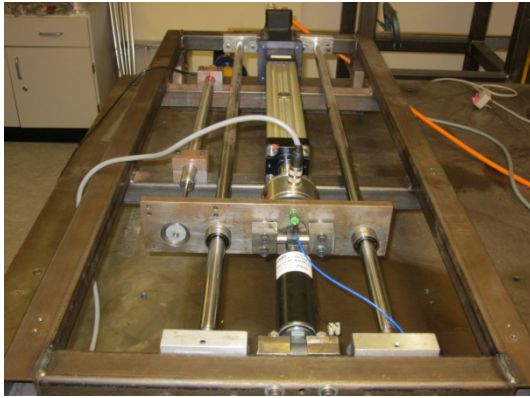
a) Displacement response b) Enlarged view of displacement response
 Figure 5.4 Displacement response of damper specimen



a) Velocity response b) Enlarged view of velocity response
 Figure 4.5 Seismic response of damper specimen

5. EXPERIMENTAL VERIFICATION

The validation test of single degree of freedom structure with MR damper is carried out at ACTlab of Engineering faculty in University of Bristol. The pictures of test rig are shown as Fig. 5.1.



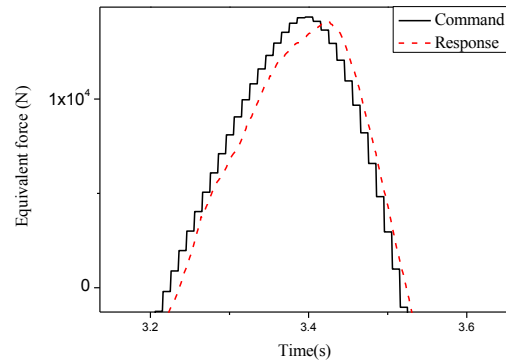
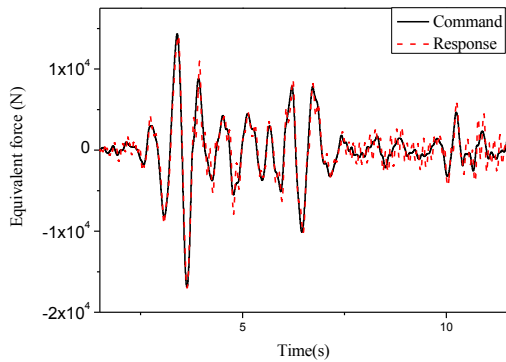
a) Experimental rig set-up of substructured model

b) Enlarged view of the specimen

Figure 5.1 Experimental rig set-up of substructured model

The amplifier of the force sensor is the Modular 600 Multi-Channel Signal Conditioning System provided by RDP Corporation. And the force sensor is RLU01000 tension and compression sensor provided by RDP Corporation, its full scale is $\pm 10\text{kN}$. The maximum force of MR damper is $\pm 1\text{kN}$. So the force sensor configuration is reasonable. The parameters of the single degree of freedom structure are: $M_N=720\text{kg}$, $K_N=74400\text{N/m}$, $\zeta_N=0.05$, $M_E=0$. The natural frequency was 1.1679Hz . The time step interval was 0.01s . The force-displacement conversion matrix was chosen $C_F=(C_N+C'_E+\frac{2M_N}{\Delta t})^{-1}\text{s}^{-1}$, in which the damping of the numerical substructure and experimental substructure were the same $C_N+C'_E=0.2M_N\omega$. Proportional feedforward controller was used as the actuator controller, with the parameters $k_p=22$ and $k_{ff}=1.08$. And the PI controller was used as the equivalent force controller, with the parameters $k_p=1$, $k_i=20$. RD-1105-3 from the Lord Corporation is chosen as the MR damper. 0V voltage was input to MR damper. The parameters of adaptive prediction compensation are: $P=4.4$, $k_a=1.03$, $\alpha=100$, $\beta=5$, $g=10^{-5}$, $\gamma=2$.

The seismic responses of explicit equivalent force control method are shown as Fig.5.2, and Fig.5.3. The maximum acceleration is 12.5 gal . The parameters of equivalent force controller are: $k_p=1$, $k_i=10$. The parameters of adaptive prediction compensation are: $P=3.5$, $k_a=1.17$, $\alpha=100$, $\beta=5$, $g=0.5 \times 10^{-5}$, $\gamma=2$.

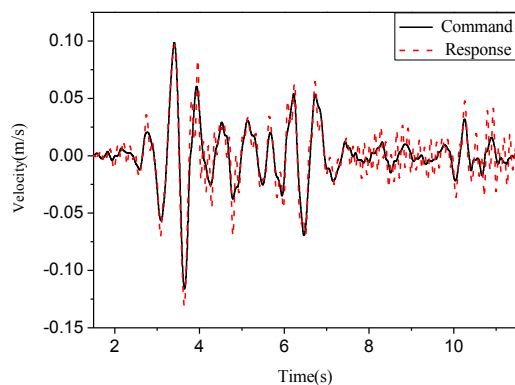


a) Equivalent force response

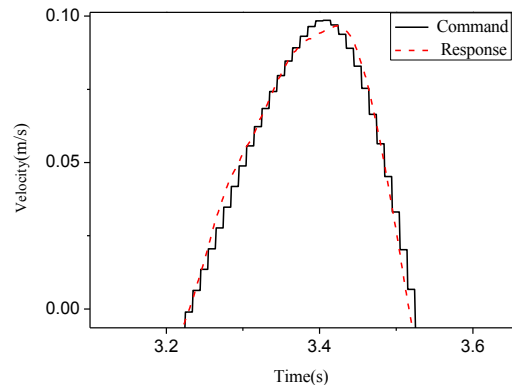
b) Enlarged view of equivalent force response

Figure 5.2 Equivalent force response

It can be seen from Figure 5.2 that the equivalent response track the command very well in spite of the noise and fluctuate. This is caused by the noise in velocity response. According to Figure 5.3, the velocity response dovetailed with the command very well, the test results prove its feasibility.



a) Velocity response



b) Enlarged view of velocity response

Figure 5.3 Velocity response with earthquake input

6. CONCLUSION

This paper proposed the explicit equivalent force control method to achieve control targeting at velocity. PI control is used to design the equivalent force controller of this method. Numerical simulation of the real-time substructure testing of the specimen with MR damper is carried out. 1) The spectral radius analysis indicates that the stability limit of this method is greater than that of central difference method using linear interpolation; 2) For cases of substructures with damping coefficients greater than 1, the stability limit of the explicit equivalent force control method is greater than that of implicit equivalent force control method using linear interpolation. 3) The results of the experiment demonstrated that the proposed method can control both the displacement and velocity of the damper accurately.

REFERENCES

1. Nakashima M, Kato H, Takaoka E. Development of Real-time Pseudodynamic Testing[J]. *Earthquake Engineering and Structural Dynamics*, 1992, 21(1):79—92.
2. Gui Y, Wang J, Jin F, Chen C, Zhou M. Development of a family of explicit algorithms for structural dynamics with unconditional stability[J]. *Nonlinear Dynamic*, 2014, 77:1157—1170.
3. Bursi O S, Jia C, Vulcan L, et al. Rosenbrock-based algorithms and subcycling strategies for real-time nonlinear substructure testing[J]. *Earthquake Engineering and Structural Dynamics*, 2011, 40:1—19.
4. Wu B, Xu G S, Wang Q Y, et al. Operator-splitting Method for Real-time Substructure Testing[J]. *Earthquake Engineering and Structural Dynamics*, 2006, 35:293—314.
5. Chen C, Ricles J M. Stability analysis of explicit integration algorithms with actuator delay in real-time hybrid testing[J]. *Earthquake Engineering and Structural Dynamics*, 2008, 37:597—613.
6. Wu B, Bao H, Ou J, et al. Stability and accuracy analysis of central difference method for real-time substructure testing[J]. *Earthquake Engineering and Structural Dynamics*, 2005, 34(7):705—718.
7. Darby A P, Blakeborough A, Williams M S. Improved control algorithm for real-time substructure testing[J]. *Earthquake Engineering and Structural Dynamics*, 2001, 30:431—448.
8. Wu B, Wang Q Y, Shing P B, et al. Equivalent Force Control Method for Generalized Real-time Substructure Testing with Implicit Integration[J]. *Earthquake Engineering and Structural Dynamics*, 2007, 36:1127—1149.
9. Wu B, Zhou H. Sliding Mode Control for Real-time Hybrid Test. *Structure Control and Health Monitoring*, 2014, 21(10):1284—1303.
10. Stoten D P. Fusion of kinetic data using composite filters[J]. *Proceedings of the Institution of Mechanical Engineers, Part I: Journal of Systems and Control Engineering*, 2001, 215(483):483—497.
11. Zhou H, Wu B, Wagg D J, et al. Equivalent force control with adaptive forward prediction for real-time hybrid simulation[C]. *Sixth World Conference on Structural Control and Monitoring - 6WCSCM*, Barcelona, Spain 15-17 July 2014, No:79.